Thermochemical Liquefaction of Pomace Using Sub/Supercritical Ethanol: an Integrated Experimental and Preliminary Economic Feasibility Study

Oseweuba Valentine Okoro[1] · Lei Nie[1,2] · Jehan Waeytens[3] · Masoud Hamidi[1,4] · Amin Shavandi[1]

Abstract

Fossil sourced chemicals such as aromatics, are widely employed in the chemical industry for the production of commodity items. Recognizing the un-sustainability of existing approaches in the production of these chemicals, the current study investigated the valorization of apple pomace (AP) for their production. The present study assessed AP valorization by imposing variations in processing conditions of temperature (100–260 °C), time (0.5–12 h), alcohol/water ratio v/v (0:1–1:0), and Fe^{3+}/H_2O_2 molar ratio (10:1–100-1), in accordance to the Box-Behnken experimental design. The optimal yield of the oil was 24.6 wt.%, at the temperature, time, alcohol/water ratio v/v, and Fe^{3+}/H_2O_2 molar ratio of 260 °C, 4.7 h, 1, and 100, respectively. Notably, the application of gas chromatography-mass spectroscopy showed that the oil product contained mainly aromatics and interestingly also alkanes, indicating that the experimental conditions imposed promoted secondary hydrogenation reactions of oxygen-containing species during AP valorization. A consideration of the comparative economics of the proposed AP valorization and the existing AP management approach, using approximate estimation techniques, highlighted the potential of a ~ 59% reduction in the unit cost of AP management. The study therefore presents a compelling basis for future investigations into AP waste management using the thermochemical liquefaction technology.

Keywords Box-Behnken · Waste valorisation · Optimization · Biorefinery

Introduction

The apple processing industry is characterized by the generation of post-harvesting waste [1]. This waste stream is referred to as apple pomace (AP) [2] and constitutes a substantial biomass resource with ~ 10 million tons generated annually from the apple juice sector [3]. The valorization of AP has therefore been recognized as a viable pathway for the production of high-value products such as succinic acid, lactic acid, and xylitol via the transformation of its polysaccharide content [4]. However, while value extraction from AP via carbohydrate transformation has been previously investigated, no study has thus far explored the potential of valorizing the lignin content of AP for high-value outcomes. Lignin is the second most abundant biopolymer on earth [5] and accounts for 15.3–23.5wt.% [6, 7] of AP. Unfortunately, in spite of lignin's abundance, there is a historical misconception that lignin presents a poorer valorization opportunity. Indeed, the potential of

✉ Oseweuba Valentine Okoro
   oseweuba.okoro@ulb.be

✉ Amin Shavandi
   amin.shavandi@ulb.be

   Lei Nie
   nielei@xynu.edu.cn

1   Université Libre de Bruxelles (ULB), École polytechnique de Bruxelles - 3BIO-BioMatter unit, Avenue F.D. Roosevelt, 50 - CP 165/61, 1050 Brussels, Belgium

2   College of Life Sciences, Xinyang Normal University, Xinyang 464000, China

3   Boulevard du Triomphe, Université Libre de Bruxelles (ULB), Faculté des sciences, Structure et fonction des membranes biologiques, CP206/2, 1050 Brussels, Belgium

4   Department of Medical Biotechnology, School of Paramedicine, Guilan University of Medical Sciences, Rasht, Iran

lignin constituting a renewable and sustainable natural resource is consistently ignored in existing biorefinery systems, since it is typically combusted as an energy source. Recognizing the limitations of existing approaches, the present study, seeks to explore the in-situ valorization of lignin (i.e. while still in the AP matrix) to produce high-value aromatics. The study will seek to enhance the yield of aromatics by employing techniques that promote the cleavage of β-ether bonds between lignin molecules and stabilization of aromatic radicals produced, as reported in the literature [8, 9]. For instance in the study by Parsell et al., [10], aromatics were produced from raw lignin via catalyzed hydrogenolysis using pressurised H_2 at 35 bar, in the presence of Zn-Pd/C catalyst. The study showed that at the optimal temperature of 225 °C, an enhanced yield of aromatics, specifically, lignin monomers of 54 wt.%, was achieved [10]. Similarly, in another study, Song et al. [11] employed methanol as both the reaction solvent and the hydrogen source. In that study, the valorization of native birch wood lignin was investigated for the production of monomeric phenols of 4-n-propylguaiacol and 4-n-propylsyringol with yields of 36 wt.% and 12 wt.% reported, respectively. These yields were obtained at the temperature of 200 °C, after 6 h of reaction and under the action of nickel-based catalysts.

In a similar approach, the present study will employ ethanol as the hydrogen source to enable in-situ lignin valorization, since ethanol is renewable and presents a lower supercritical temperature (243.2 °C) compared to other biomass-sourced alcohols (i.e. 1-butanol, 287.2 °C) [12]. Furthermore, ethanol is capable of facilitating the scavenging of the unwanted decomposition side products such as formaldehyde thus enhancing the potential of higher yields of phenolic monomers [13]. To enhance preferential lignin depolymerization for aromatic compound production, the AP will also be pretreated using Fe^{3+}/H_2O_2 [8, 14, 15]. This investigation of the liquefaction of AP is yet to be presented in the literature. Having undertaken the AP valorization, the economic viability of the liquefaction process will also be assessed by undertaking a preliminary comparative study. This preliminary economic study will determine the "cost potential" of the proposed AP liquefaction strategy when scaled-up. The combined assessment of the potential for the production of valuable chemicals from AP and the economic viability of a scaled-up system contributes to the novelty of the present study.

Materials and Methods

Sample Preparation

The fresh AP was sourced locally from Materne-Confilux Company (Namur, Belgium) in February 2021. The acquired samples were initially mixed to ensure homogeneity and then dried to constant mass at 60 °C for 24 h. The dried AP samples were then finely ground and sieved using a 0.5 mm Endecott mesh. The composition of the AP (67.3 ± 1.06 wt.% moisture) was reported in our earlier study [7] and presented in Table 1.

Table 1 summarizes the macromolecule composition and the proximate and ultimate analyses results of the dry AP. The dry AP samples were then stored using airtight polythene bags and preserved in a freezer at a temperature of −18 °C. Additionally, chemical inputs of $Fe_2(SO_4)_3$ (Reagent grade VWR Chemicals, Belgium), H_2O_2 (analytical grade, Chemical Lab, Belgium), dichloromethane (Reagent grade VWR Chemicals, Belgium), and C_2H_5OH (Reagent grade VWR Chemicals, Belgium), were also used.

Process Variables Explored

The variables of temperature, time, and alcohol-water volume ratio were initially selected since they have been reported to influence aromatic compound yield during liquefaction reactions [8, 16–18]. Further review of published works also highlighted that temperature and time ranges of 100–260 °C and 0.5–12 h respectively were sufficient [10, 19–24]. Furthermore, the temperature range specified in the current study is lower than the temperatures of conventional hydrothermal liquefaction processes (i.e. > 300 °C) [25] since it is hypothesized that lower temperatures will limit the transformation of other major components of apple pomace i.e. carbohydrate and proteins possibly via Maillard and free radical reactions respectively [26, 27]. The ethanol–water mixing ratios of 0:1 and 1:0 (volume basis) were considered the lower and upper limits respectively in this study. Since hydrogen peroxide contributes substantially to the overall cost in oxidation processes, Fe^{3+}/H_2O_2 molar ratios were investigated using excess Fe^{3+}. Therefore,

Table 1 Composition of the apple pomace (AP) (wt.%, dry AP basis) [7]

Characterisation	Measured value
Lipid content	1.29 ± 0.52
Carbohydrate content	71.9 ± 1.30
Protein content	5.94 ± 0.20
Lignin content	19.5 ± 1.18
Ash content	1.30 ± 0.00
Volatile content	92.4 ± 0.00
Fixed carbon	6.34 ± 0.00
Carbon content	46.1 ± 0.64
Hydrogen content	6.87 ± 0.11
Nitrogen content	0.95 ± 0.03
Oxygen content	46.0 ± 0.65
Sulphur content	0.07 ± 0.01

0.5 M of $Fe_2(SO_4)_3$ and separate solutions of 0.05 M and 0.005 M of H_2O_2 were prepared and employed to achieve Fe^{3+}/H_2O_2 molar ratios of 100:1 and 10:1, as the upper and lower molar ratio limits respectively.

Experimental Design and Statistical Analysis

The current study explored the effects of process variables on oil yield and also determined the appropriate conditions for optimal oil yield using the Box-Behnken experimental design approach [28]. Table 2 therefore provides the process variables and their coded levels and actual values.

The values of the coded levels of the variables were determined as follows [29];

$$x_i = \frac{X_i - X_0}{\Delta X} \quad (1)$$

where x_i represents the coded level of the ith process variable; X_i is the actual value of the ith process variable; X_0 denotes the actual value of X_i at the center point, with the step change value denoted as ΔX.

Having employed the Box-Behnken design, 27 experimental runs were undertaken and the results analyzed using Minitab® 17.1.0 (Minitab, Inc. USA). The results were subsequently correlated to a second order response as follows;

$$Y_{oil} = X_0 + \sum_{i=1}^{4} b_i X_i + \sum_{i=1}^{4} b_{ii} X_i^2 + \sum_{i=1}^{4} \sum_{j=1}^{4} b_{ij} X_i X_j \quad (2)$$

where Y_{oil} denotes the yield of the oil product in wt.%, X_o represents the model intercept, X_i (X_j) represents the ith (jth) system variable (temperature, time, Fe^{3+}/H_2O_2 molar ratio, or alcohol/water ratio v/v), b_i, b_{ii}, and b_{ij} represent the model regression coefficients.

Further analysis of the data was undertaken to determine the significance of different process variables on oil yield. The current study assessed the value of the student F-value of each variable rel*ativ*e to the critical F-value (3.13) of the experimental data, such that the magnitude of student F-value > critical F-value was indicative of the significance

of the variable [30]. The significance was further demonstrated when the p-value was less than 0.05 for a 95% confidence interval [31]. The process conditions that facilitate optimal oil production were subsequently determined.

Experimental Procedure

Ten grams of the dried AP sample was initially added to 100 mL of Fe^{3+}/H_2O_2 according to molar ratios specified in the experimental design (Table 2) and the resulting solution rigorously stirred at 120 rpm for 1 h at 60 °C temperature [14]. After mixing, the treated sample was recovered using vacuum filtration and the recovered solids thoroughly washed using distilled water. The treated AP was then dried to constant mass at 60 °C for 24 h. 1 g of the dried and treated AP sample was added to the solvent mixture of ethanol and water (10 mL), then introduced to the reactor and sealed. The reactor (Henan Lanphan Industry Co., Ltd, Zhengzhou, China) was a 304 stainless steel autoclave reactor, equipped with a proportional-integral-derivative (PID) temperature controller and a J-type thermocouple. Air in the reactor was initially purged using nitrogen for 3 min and inlet and sampling valves subsequently sealed. The conditions of the process variables were then imposed according to the specified Box-Behnken experimental design. At the end of the reaction, the reactor was rapidly cooled by immersing the reactor in an ice bath. The cooled reactor was then opened and the oil product recovered using dichloromethane as described in the literature [32].

The yield of the oil product, Y_{oil}, in wt.%, was determined as follows;

$$Y_{oil} = \frac{m_{oil} \times 100}{m_{sample}} \quad (3)$$

where m denotes the mass in g.

The oil product was then stored in a fridge at 4 °C, prior to undertaking the characterisation experiment.

Characterization Experiments

Characterization of the Oil Product

The optimally produced oil recovered was characterized via gas chromatography-mass spectroscopy (GC–MS) to identify the major compounds present in the oil. The GC–MS was undertaken using a gas chromatograph equipped with a mass selective detector (GC–MS, model Trace GC and DSQII). The injector was maintained at the temperature of 280 °C with helium employed as the carrier gas at the constant flowrate of 1.1 mL/min. A ZB-5 ms column from phenomenex (length, 30 m; internal diameter, 0.25 mm; film thickness, 0.25 µm) was utilized. For compound separation,

Table 2 Coded levels and actual values of the process variables

Parameters	Coded and actual values for the levels in the experimental design		
	Low	Center	High
Levels	−1	0	+1
Fe^{3+}/H_2O_2 molar ratio, r	10	55	100
Time, t (h)	0.5	6.25	12
Temperature, T, (°C)	100	180	260
Alcohol/water ratio, v/v, a	0	0.5	1

the oven was maintained at the temperature of 50 °C for 5 min after which a heating rate of 5 °C/min was imposed until the temperature of 300 °C was attained. The injected volume and split ratio were 1 μL and 1:10 respectively. The mass spectra was subsequently generated. The main chemical compounds present in the oil sample (i.e. percentage area > 0.2%) were subsequently determined via comparative assessments of the mass spectra of the fragmentation patterns generated and the mass spectra of compounds in the database of the National Institute of Standards and Technology.

Optimization of Yield of Oil

The conditions of the process variables that will enable the optimal production of oil were determined based on the empirical model. The conditions of the process variables were determined using the desirability-function numerical optimization module in Minitab. The experimentally determined optimal yield of the oil was subsequently compared with the yield predicted using the empirical model and then comparatively assess using the relative absolute deviation (*RAD*) metric which is defined as follows [33],

$$RAD = \frac{\left| Y_{oil,\exp} - Y_{oil,pre} \right|}{Y_{oil,\exp}} \tag{4}$$

where $Y_{oil,\exp}$ represents the experimentally determined yield of the oil (wt.%), $Y_{oil,\,pre}$ denotes the predicted yield of the oil product (wt.%).

Preliminary Economic Assessment of the Apple Pomace Liquefaction Process

To assess the economic performance of the AP liquefaction process (ALP), the methods described in the experimental section above provided the basis of the simplified flow diagram presented in Fig. 1. Briefly, Fig. 1 shows that the AP is initially pretreated using the Fe^{3+}/H_2O_2 after which the modified AP is washed using distilled water, filtered, then air dried prior to undertaking sub/supercritical ethanol liquefaction as described ealier above. At the end of the reaction, the product mixture is pumped to a filter to remove the solid residues after which a settling tank is employed in oil recovery. The present study assumes that immiscibility and specific gravity property differences of the oil and ethanol liquid phase will be sufficient to enable the recovery of the oil phase in large-scale operations since a similar assumption regarding the gravity separation of oil and aqueous solutions was employed in previous works [34, 35]. For simplicity, it is also assumed that the ALP operates in steady-state.

To undertake the a comparative economic assessment, estimates were generated and utilized in the calculation of the unit cost of the ALP (U_l) compared to existing unit cost of AP management (U_m). The existing cost of AP management was specified as US$ 10 million to process 200.68 tons (dry basis, with moisture content of 67.3 wt.% assumed) AP per year [36]. This AP management cost, U_m, translates to US$ 49.8 per kg (dry AP basis). The moisture content of the AP was specified as 67.3 wt.% to ensure similarity with experimentally determined moisture content in the present study. Therefore, for an equal dry mass of AP and assuming the ALP plant operates for 7200 h per year, the U_l in US$ per kg (dry AP basis) was determined as follows [34];

$$U_l = \frac{C_i}{m_{AP}} \tag{5}$$

$$C_i = C_{AC} + C_{OC} \tag{6}$$

$$C_{AC} = I_j \times \left[\frac{(1+i)^n \times i}{(1+i)^n - 1} \right] \tag{7}$$

$$I_j = 1.81 \times E_{ISBL,j} \tag{8}$$

$$E_{ISBL,j} = f_L \sum_i^n Cost_{i,j} \tag{9}$$

where C_i, C_{AC}, and C_{OC} denote the total cost (US$), annualized capital cost (US$), and the annual operating cost (US$). The m_{AP} represents the mass of AP (kg) liquefied per year on the dry basis. The I_j $E_{ISBL,j}$ and f_L denote the total investment cost, inside battery limit equipment (ISBL) cost for the *j*th year and the updated lang factor of 5.04 [37] respectively. These equations also present *n*, *i*, and $Cost_{i,j}$ which denote the lifespan and discount rate of the project, assumed to be 10 years and 10% respectively and the purchase of the *i*th major equipment in the *j*th year.

For the ALP plant, the purchase cost of the sub/supercritical reactor was estimated using the scaling factor approach and based on the manufacturer quoted price of US$ 1445 per 250 mL processing capacity (Henan Qiuzuo Instrument and Equipment Co., Ltd, China, quoted price). Also, each cooler was assumed to be a heat exchanger with an average cost of US$ 3000 (Luoyang Zhengyuan Petrochemical, China, quoted price). The purchase cost of the settling tank was also specified as US$23283.21 for 100 m³ of mixture based on year 2006 cost estimates [34, 38].

It must be noted that differences in processing capacities were adjusted using the relation [4];

$$P_{c:i,Q} = P_{c:i,Q_{ref}} \left(\frac{Q}{Q_{ref}} \right)^a \tag{10}$$
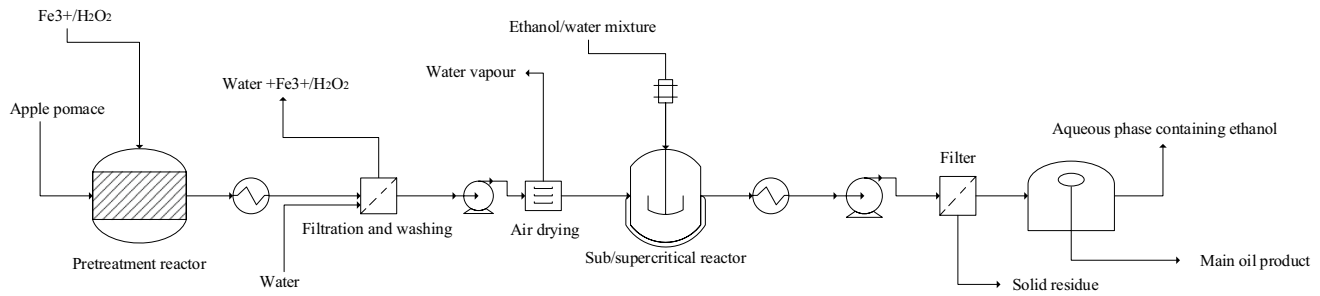
Fig. 1 Simplified flow diagram for the proposed apple pomace liquefaction process

where $P_{c:i,Q}$ and $P_{c:i,Qref}$ denote the reactor purchase costs in US$ at the desired capacity and the reference capacity respectively. Q_{ref}, Q, and a represent the reference capacity, desired capacity, and the scaling factor of 0.65 [39] respectively.

The purchase costs of the settling tank ($Cost_t$ in US$), pump ($Cost_p$ in US$), filter ($Cost_f$ in US$), and pretreatment reactor ($Cost_r$ in US$) were calculated as follows [34, 38];

$$Cost_t = 5700 + 700v_t^{0.7} \qquad (11)$$

$$Cost_p = 3300 + 48v_p^{1.2} \qquad (12)$$

$$Cost_f = -45000 + 56000A_f^{0.3} \qquad (13)$$

$$Cost_r = 13000 + 34000v_r^{0.5} \qquad (14)$$

where in Eqs. (11)–(14), v_r, v_p, A_f, and v_t denote the volume of the feed processed in the pretreatment reactor (m³ per h), volume flow rate (L/s) through the pump, assumed area of the filter specified as 20 m² and assumed volume of the settling tank was specified as 10 m³. The density of the dry AP was specified as 520 kg/m³ [39]. The constants, 5700, 700, 0.7, 3000, 48, −45,000, 56,000, −14,000, 15,400, 0.3, and 1.2, denote the Towler and Sinnot correlation cost constants based on year 2006 cost estimates, respectively. An adjustment factor of 1.2 has also been imposed on the estimated volumes, to allow for 'overhead space' in the vessels.

To account for the inflationary effects of money on the cost, the equipment purchase cost was adjusted to provide year 2022 estimates using the chemical engineering plant cost index (CEPCI) as follows [4];

$$P_{c:i,2022} = P_{c:i_{ref}} \left(\frac{CEPCI_{2022}}{CEPCI_{ref}} \right) \qquad (15)$$

where the ith equipment purchase costs in the year 2022 and the reference year of 2006 are denoted by $P_{c:i,2022}$ and $P_{c:i,ref}$

with CEPCI's specified as 776.9 and 499.6 in www.chemengonline.com, respectively.

To estimate the C_{OC}, the labor, energy, depreciation, overhead, and maintenance/repair costs were determined and added. The hourly labor wage was assumed to be US$ 23.44 per h for each of the 3 onsite workers (www.payscale.com). For simplicity, Eq. (15) was used to calculate the heat duty of the scaled-up reactor relative to the reference heat duty (0.8 kW) of the bench-scale reactor used in the experimental investigation.

The energy input, $\dot{E}_h$, in kJ/h consumed during the AP pretreatment was estimated as follows [41];

$$\dot{E}_h = \left[\dot{m}_{solu}\left(c_{solu}(T°C - 25)\right) + \left(\dot{m}_{AP}c_{AP}(T°C - 25)\right) \right] \qquad (16)$$

where c_{solu} and c_{AP} represent the specific heat capacities of the solution of Fe^{3+}/H_2O_2 and dry AP assumed to be 4.18 kJ/kg·C (since the solution of Fe^{3+}/H_2O_2 is composed of mainly water) and 1.25 kJ/kg·C for biomass, respectively [42]; $\dot{m}_{solu}$, $\dot{m}_{AP}$, and $T°C$ denote the mass flow rate of the solution in kg/h, the mass flow rate of dry AP in kg/h, and the heating temperature of 60 °C respectively.

The unit heat energy cost was specified as US$ 0.0681 per kWh [34] which constitutes the pre-COVID-19 value. The depreciation cost was estimated by assuming linear depreciation for a period of 10 years with a salvage value of zero specified. The maintenance/repair cost was calculated as 6% of the investment cost while the overhead cost (OV_c) was estimated as the follows [34, 43];

$$OV_c = 0.05\left(dep_c + La_c + En_c\right) \qquad (17)$$

where dep_c, La_c, and En_c denote the annual depreciation, annual labor, and annual energy costs in US$, respectively.

Finally, the costs of the chemical inputs of ethanol, $Fe_2(SO_4)_3$ and H_2O_2 of US$ 0.873 per L, US$ 0.315 per kg and US$ 6.6 per kg, were obtained from commercial price websites of Globalpetrolprices.com, Alibaba.com and Pharmacompass.com respectively.

Results and Discussions

Model Fitting

Table 3 shows the conditions of the process variables imposed in the present study with each oil yield presented as mean value ± standard error. Table 3 shows that the oil yield varies from 3 to 23.3 wt.% and the SR yield varies from 18.75 to 69.89 wt.%. It is also observed that the highest oil yield of 23.30 wt.% is achieved at time (t), alcohol/water volumetric ratio (a), temperature (T), and Fe^{3+}/H_2O_2 molar ratio (r) of 6.25 h, 1, 260 °C, and 100 respectively. A consideration of the results suggests that higher temperatures and longer reaction times favor higher oil yields.

This observation is expected since at low temperatures and shorter reaction times, biomass depolymerization reactions are less likely to occur. Employing Minitab, empirical relationship between oil yield (Y_{Oil}) and process variables was determined as follows;

$$
\begin{aligned}
Y_{Oil} = &-20.2 + 3.577t - 0.4a + 0.2678T - 0.033r \\
&- 0.1463t^2 - 7.65a^2 - 0.000650T^2 \\
&- 0.000772r^2 + 0.790t \times a - 0.01283t \times T \\
&+ 0.00335t \times r + 0.0695a \times T + 0.0106a \times r \\
&+ 0.000639T \times r
\end{aligned}
\tag{18}
$$

where Y_{oil} denotes the yield of the oil; t, a, T, and r denote the time (h), alcohol/water v/v ratio, temperature (°C), and Fe^{3+}/H_2O_2 molar ratio, respectively.

The empirical model shown in Eq. (18) is characterized by a coefficient of correlation (R^2) value of 0.8549. This R^2 value exceeds the value of 0.7 which was previously reported as the minimum acceptable R^2 value that characterizes general scientific studies [44].

Model Statistics Analysis

Using Minitab, the model describing oil yield was assessed via analysis of variance (ANOVA), with the results shown in Table 4. Table 4 shows that the empirical model describing the dependence of oil yield on the process variables has high statistical significance as illustrated by the model F-value of 5.05 that is greater than the critical F-value of 3.13. This observation is expected given the high correlation coefficient of 0.8549. It is also observed that the alcohol/water v/v ratio constitutes the most significant parameter that influences oil yield in the present study. This is because, the process variable of alcohol/water ratio has an F-value of 28.61, which is greater than the critical F-value of 3.13 of the model. The significance of other process variables on oil yield were $T > Fe^{3+}/H_2O$ and $r > t$, as illustrated by their F-values. Notably, Table 4 also shows that the interaction effects of time and temperature (i.e., $t \times T$)

constituted the most important interaction that influences oil yield in the current study with the F-value of 12.00. This observation implies that the effects of temperature on oil yield becomes more dominant as the reaction time increases.

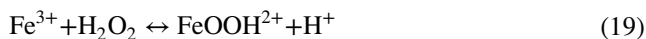### Effects of Process Variables

Figure 2 shows the statistically average independent effects of the process variables on the oil yield using two-dimensional planar plots. Figure 3 shows the three-dimensional surface plots highlighting the combined effects of the process variables on the oil yield. These effects are discussed in subsequent sections.

Effect of Temperature

Figure 2 shows that there is an initial positive correlation between oil yields and increasing temperatures. However, beyond the temperature of 180 °C, oil yields are observed to reduce. This observation is expected since reaction kinetics suggests that higher temperatures will present favorable effects on depolymerization reactions via the enhanced cleavage of bonds. Additionally, since liquid ethanol becomes more nonpolar as the reaction temperature approaches its critical temperature, while retaining its hydrogen-bond donating ability, it is expected that higher temperatures will facilitate enhanced AP solvolysis and lignin hydrogenolysis [45]. These favorable effects of temperature are however not maintained since temperatures greater than 180 °C lead to lower oil yields, thus highlighting the thermal instability of the oil at higher temperatures.

Effect of Fe^{3+}/H_2O_2 Molar Ratio

Figure 2 shows that increments in the Fe^{3+}/H_2O_2 molar ratio from 10 to 100 leads to a 16% increase in oil yields. This observation may be due to the effects of biomass oxidation under the action of free radicals (i.e. HOO, Eqs. (19)–(26) [46]) and iron-lignin/biomass complex formation during pomace preparation [14].

$$Fe^{3+} + H_2O_2 \leftrightarrow FeOOH^{2+} + H^+ \tag{19}$$

$$FeOOH^{2+} \rightarrow Fe^{2+} + HOO^\bullet \tag{20}$$

$$Fe^{2+} + H_2O_2 \rightarrow Fe^{3+} + HO^- + HO^\bullet \tag{21}$$

$$HO^\bullet + H_2O_2 \rightarrow H_2O + HOO^\bullet \tag{22}$$

Table 3 Oil yields at different conditions of the process parameters

N	Coded values of parameters				Actual values of parameters				Y_{Oil} (wt.%)
	t (h)	a	T (°C)	r	t (h)	a	T (°C)	r	
1	+1	0	0	−1	12	0.5	180	10	12.62 ± 1.94
2	0	−1	0	−1	6.25	0	180	10	8.26 ± 1.83
3	+1	0	−1	0	12	0.5	100	55	10.00 ± 1.00
4	−1	+1	0	0	0.5	1	180	55	9.80 ± 0.01
5	+1	+1	0	0	12	1	180	55	18.80 ± 0.02
6	−1	0	0	−1	0.5	0.5	180	10	13.33 ± 0.00
7	+1	0	0	+1	12	0.5	180	100	16.49 ± 0.02
8	0	+1	0	+1	6.25	1	180	100	23.16 ± 2.10
9	+1	0	+1	0	12	0.5	260	55	5.10 ± 0.02
10	0	0	−1	−1	6.25	0.5	100	10	12.09 ± 2.20
11	0	+1	0	−1	6.25	1	180	10	21.90 ± 2.86
12	−1	0	−1	0	0.5	0.5	100	55	3.00 ± 0.00
13	0	−1	−1	0	6.25	0	100	55	11.00 ± 0.01
14	−1	0	0	+1	0.5	0.5	180	100	13.73 ± 0.01
15	0	0	0	0	6.25	0.5	180	55	18.00 ± 2.15
16	0	0	0	0	6.25	0.5	180	55	20.00 ± 3.16
17	0	+1	−1	0	6.25	1	100	55	16.32 ± 2.04
18	0	0	−1	+1	6.25	0.5	100	100	10.75 ± 1.10
19	0	0	+1	+1	6.25	0.5	260	100	18.28 ± 1.10
20	+1	−1	0	0	12	0	180	55	9.38 ± 0.00
21	−1	−1	0	0	0.5	0	180	55	9.47 ± 1.10
22	0	−1	+1	0	6.25	0	260	55	6.86 ± 0.01
23	0	0	+1	−1	6.25	0.5	260	10	10.42 ± 1.04
24	0	+1	+1	0	6.25	1	260	55	23.30 ± 3.88
25	−1	0	+1	0	0.5	0.5	260	55	21.7 ± 2.83
26	0	−1	0	+1	6.25	0	180	100	8.57 ± 1.90
27	0	0	0	0	6.25	0.5	180	55	20.00 ± 0.07

$$HO_2^\bullet \leftrightarrow H^+ + O_2^{\bullet -} \tag{23}$$

$$O_2^{\bullet -} + Fe^{3+} \rightarrow Fe^{2+} + O_2 \tag{24}$$

$$2HO_2^\bullet \rightarrow H_2O_2 + O_2 \tag{25}$$

$$Fe^{2+} + 2HO_2^\bullet \rightarrow Fe^{3+} + HO_2^- \tag{26}$$

Notably, Fig. 2 also shows that the effect of increasing Fe^{3+}/H_2O_2 molar ratio from 55 to 100 on the oil yield (12.2%) is more impactful than the effect of increasing Fe^{3+}/H_2O_2 molar ratio from 10 to 55 on oil yield (3.14%). This observation may be indicative of the "stronger" role of Fe^{3+}-lignin complex formation in the dry AP, compared to the effect of free radical oxidation on oil production. This may be because of the reduced potential for HOO· formation due to the low concentration of H_2O_2 employed. The favorable effects of higher Fe^{3+}/H_2O_2 molar ratios on oil yield may also be because, any biomass–iron chelating complexes formed, can act as capping agents which limit intramolecular condensation reactions for unwanted char formation [8].
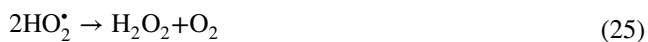
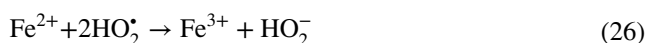### Effect of Alcohol/Water Volumetric Ratio

Figure 2 shows that a positive correlation exists between oil yields and increasing alcohol/water v/v ratios. This is because a higher fraction of ethanol in the solvent mixture presents enhanced opportunities for AP solvolysis due to the near non-polar properties of ethanol observed as the critical temperature of ethanol is reached. Such polarity changes may however not be observed in the water fraction of the solvent since the critical temperature of water is higher than the critical temperature of ethanol. Thus, the higher the fraction of ethanol in the solvent mixture, the higher the potential for solvolysis and hydrogenolysis, since more hydrogen (from the alcohol) is made available for the cleavage of bonds.

Table 4 The significance of the operational variables on the oil yields

Source	DF	Adj SS	Adj MS	F-value	p-value	Remarks
Model	14	734.695	52.478	5.05	0.004	**
t	1	0.154	0.154	0.01	0.905	*
a	1	297.406	297.406	28.61	0.000	**
T	1	42.187	42.187	4.06	0.067	*
r	1	12.731	12.731	1.22	0.290	*
t^2	1	124.743	124.743	12.00	0.005	**
a^2	1	19.482	19.482	1.87	0.196	*
T^2	1	92.352	92.352	8.88	0.011	**
r^2	1	13.042	13.042	1.25	0.285	*
$t \times a$	1	20.657	20.657	1.99	0.184	*
$t \times T$	1	139.240	139.240	13.40	0.003	**
$t \times r$	1	3.010	3.010	0.29	0.600	*
$a \times T$	1	30.914	30.914	2.97	0.110	*
$a \times r$	1	0.226	0.226	0.02	0.885	*
$T \times r$	1	21.160	21.160	2.04	0.179	*
Error	12	124.731	10.394			
Lack-of-fit	10	122.065	12.206	9.15	0.102	*
Pure error	2	2.667	1.333			
Total	26	859.426				

*Low significance, i.e., F-value < 3.13, **high significance, i.e., F-value > 3.13; *DF*, degrees of freedom; t, T, a, and r denote time, temperature, alcohol/water v/v ratio, and Fe^{3+}/H_2O_2 molar ratio respectively.

Fig. 2 Statistical independent effects of the process variables on the oil yield generated
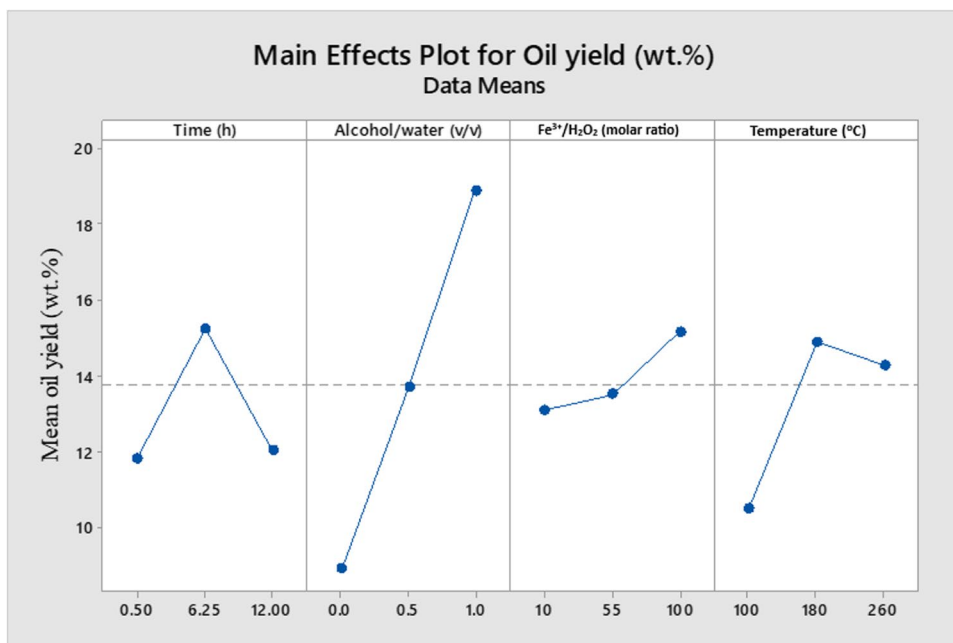

Effect of Reaction Time

Figure 2 shows that longer reaction times initially translates to higher oil yields with a decrease in the oil yield observed when the reaction time exceeds 6.25 h. This result suggests that while a sufficient reaction duration is required for oil generation, long reaction times (> 6.25 h) increases the risk of oil decomposition.

Combined Effects of the Process Variables on Responses

The combined effects of the process variables are highlighted in Fig. 3. Figure 3a, c, and f highlight the effects of interactions between alcohol/water v/v ratio and the parameters of time, temperature, and Fe^{3+}/H_2O_2 molar ratio respectively,
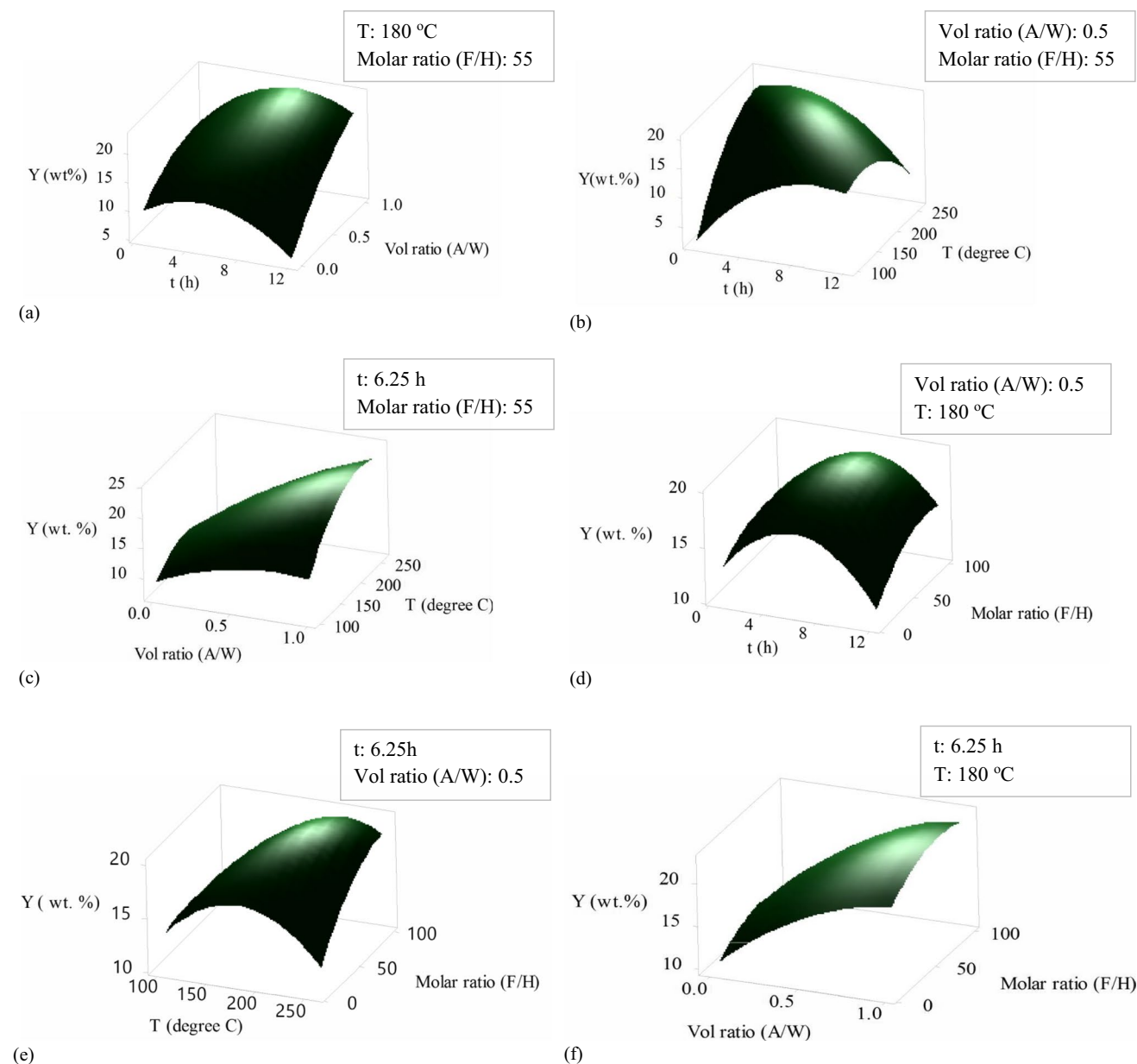
Fig. 3 Combined effects of the process variables on the oil yield. Values of the process variables held constant are presented in legends. Herein, t, T, vol ratio (A/W), and molar ratio (F/H) denote time (h), temperature (°C), alcohol/water v/v ratio, and Fe^{3+}/H_2O_2 molar ratio respectively

on oil yield. Figure 3a shows that simultaneously increasing alcohol/water v/v ratio (0 to 1) and increasing time (0.5 h to 12 h) lead to net positive effects on oil yield. This observation emphasizes the dominance of the effects of alcohol/water v/v ratio on the product yield as highlighted by the ANOVA results since the positive effects of alcohol/water v/v ratio on product yields outweighs the negative effects of extended reaction time. Figure 3b shows the interaction effect of temperature and time on the oil yield. It shows that the effects of increasing temperature and increasing time are initially favorable. However, for long reaction times

(> 6.25 h) and higher temperatures (> 180 °C), a decrease in the oil yield is observed and is due to the thermal instability effects discussed earlier above.

Products at the Optimal Experimental Conditions

Optimization conditions for an enhanced oil yield was determined using the Minitab software and based on the empirical model. It was determined that the optimal conditions of temperature (260 °C), time (4.7 h), alcohol/water v/v ratio (1:0), and Fe^{3+}/H_2O_2 molar ratio (100) facilitated the predicted

Table 5 Major compounds detected in the oil product

Compound name	Chemical abstracts service registry number	Apex retention time (min)	Chemical formula	Molecular weight (kg/kmol)	Normalized area percentage
Toluene	108–88-3	3.23	C_7H_8	92.14	1.75
Ethylbenzene	100–41-4	5.56	C_8H_{10}	106.16	1.35
m-xylene	108–38-3	5.84	C_8H_{10}	106.16	1.89
5-Hydroxymethylfurfural	67–47-0	19.05	$C_6H_6O_3$	126.11	2.02
2,6-dihydroxyacetophenone	699–83-2	19.48	$C_8H_8O_3$	152.15	0.34
Phthalic anhydride	85–44-9	20.72	$C_8H_4O_3$	148.1	0.33
4-hydroxybenzaldehyde	123–08-0	21.51	$C_7H_6O_2$	122.123	0.40
Vanillin	121–33-5	22.92	$C_8H_8O_3$	152.15	1.11
6-methoxy-2,3-dihydrobenzofuran-2-carboxylic acid	41,910–91-2	31.4	$C_{10}H_{10}O_4$	194.18	0.47
Phthalic acid	88–99-3	34.44	C_8H_6O	166.13	0.63
Octadecanoic acid hexyl ester	3460–37-5	44.11	$C_{24}H_{48}O_2$	368.64	0.25
n-Eicosane	112–95-8	48.27	$C_{20}H_{42}$	282.5	77.18
Methyl oleanonate	112–62-9	51.63	$C_{19}H_{36}O_2$	296.5	10.28
Cyclohexyl ester	1551–41-3	52.73	$C_{15}H_{28}O_2$	240.3816	1.99

optimal oil product yield of 25.3 wt.%. The oil yield at these conditions was subsequently assessed experimentally and determined to be 24.6 wt.% which is comparable to the predicted oil yield of 25.3 wt.% with an *RAD* of 0.028. The solid residue yield at the optimal conditions was also determined to be 38.1 wt.%. The GC–MS result highlighting the major compounds present in the oil is shown in Table 5.

Table 5 shows that 14 major compounds are present in the oil product with Eicosane (alkane) determined to be the major component present in the oil product, with a percentage area of 77.2%. The presence of 5-Hydroxymethylfurfural (i.e. 2%) in the oil product also suggests that supercritical ethanol enabled the dehydration of the carbohydrates the reactor. Table 5 also shows that the oil product contains ~ 8.6% of aromatic compounds. The presence of esters (~ 13%) in the oil also suggests that side supercritical transesterification reactions between the AP lipids (1.29 wt.%) also occurred [47].

This work shows that the optimal oil yield obtained from the liquefaction of AP (24.6 wt.%) is lower than the oil yields of 65.8 wt.% and 30.1 wt.% reported from the supercritical ethanol liquefaction of other biomasses of pine wood and eucalyptus at conditions of 400 °C, 2 h, and 300 °C, 1 h, respectively [48, 49]. Apart from the compositional differences of the feedstocks, differences in the reaction conditions and pretreatment approaches (i.e. Fe^{3+}/H_2O_2 modification) may also explain the differences in oil yields. Specifically, the present study sought to encourage the conversion of AP lignin for enhanced aromatic compound production, via the imposition of lower temperatures and the application of an AP pre-treatment strategy. Interestingly, while the oil product was (qualitatively) determined to be composed of only ~ 8.6% of aromatic compounds, the high content of alkanes (77.2%)

constituted an unexpected outcome. Indeed, in previous studies, the alkane content of the oil product produced from liquefaction reactions was reported to range from 9 to 13% [50]. The high alkane and low aromatic compound contents of the oil in the present study may be indicative of the presence secondary hydrogenation reactions that lead to the reduction of oxygen-containing functionalities in the oil product [51]. This implies that a converse relation may exist between the yields of oxygen-containing aromatics and alkanes. It is therefore hypothesized that it is possible to further enhance the aromatic compound content of the oil by reducing the concentration of H_2 available (i.e. from the sub/supercritical ethanol) and by reducing the temperature range imposed. Thus, experimental designs to enhance the production of target aromatic yield rather than the overall oil yield will be explored in future studies.

Economics of the Proposed Apple Pomace Liquefaction

Employing the methods described in the "Preliminary Economic Assessment of the Apple Pomace Liquefaction Process" section, major costing components are summarized in Table 6.

Table 6 Major cost components in the proposed ALP process

Parameters	Cost
Total equipment cost (US$)	544463.37
ISBL cost (US$)	2744095.37
Total investment cost (US$)	4966812.63
Annual operating cost (US$)	3256096.74

Fig. 4 Costs of the apple pomace liquefaction process (ALP) and the existing apple pomace (AP) management approach. M denotes million
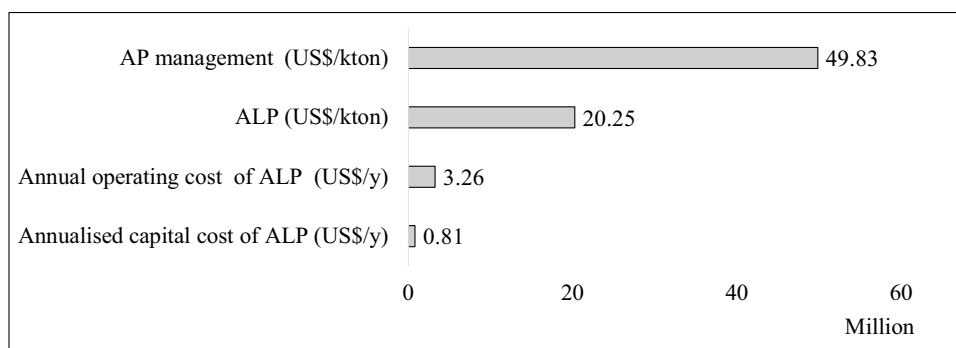
Employing the results presented in Table 6, the unit processing cost (dry mass basis) for the proposed ALP process (presented as millions US$/ktons) and the existing AP management approach (presented as millions US$/ktons) were calculated and presented in Fig. 4.

Figure 4 highlights the potential of ALP to reduce the unit processing cost of AP by ~59%. This cost reduction may however be considered as optimistic since additional expenditure due to preliminary AP air drying, contingency costs etc. have not been considered. Also, possible losses in the yield of oil due to inefficient gravity separation of oil and aqueous phases as well variations in the mass of AP, after Fe^{3+}/H_2O_2 modification were not considered. Nevertheless, the annual operating cost of ~3.3 million was estimated, with the chemical cost estimated to contribute substantially to the annual operating cost. This observation implies that further work, exploring the recovery and re-cycling of chemicals, specifically, ethanol, must be undertaken since such ethanol recovery for re-use has the potential to further enhance the economic performance. It must be stated that the costing study is limited by the underlying assumptions imposed. Although, it must be emphasized that the economic comparison methods highlighted in the present study are largely approximate, the approach herein is however supported by costing correlations in engineering plant design. It therefore implies that the methods and the associated results, although indicative, may be considered sufficient for this preliminary study.

Conclusion

In the present study, the valorization of apple pomace (AP) using sub/supercritical ethanol was investigated. The study showed that an optimal oil yield of 24.6 wt.% can be produced from AP. This oil product was determined, via qualitative approaches (% area basis), to contain mainly alkanes (77.2% area basis) and some aromatic compounds (~8.6% area basis) with a converse relation between the yields of alkanes and aromatics proposed. A preliminary economic

study also highlighted the potential of scaling up the proposed AP liquefaction process. The study was therefore able to show the possibility of producing oil containing high value alkanes and aromatics, via a one-step process, without compromising economic viability. Crucially, the study presents a compelling justification for further investigations of the transfer of the liquefaction technology to the AP waste management sector.

Author Contribution Conceptualization, O.V.O.; Methodology, O.V.O., M.H., and J.W.; Software, O.V.O. and J.W.; Validation, O.V.O., L.N., M.H., J.W. and A.S.; Original draft; O.V.O., L.N., M.H., and A.S., Supervision, L.N., O.V.O., M.H., and A.S.; Writing—review and editing, O.V.O., L.N., M.H., J.W., and A.S. All authors have read and agreed to the published version of the manuscript.

Data Availability The authors confirm that the data supporting the findings of this study are available within the article.

Declarations

Competing Interests The authors declare no competing interests.

References

1. Van Dyk JS, Gama R, Morrison D, Swart S, Pletschke BI (2013) Food processing waste: problems, current management and prospects for utilisation of the lignocellulose component through enzyme synergistic degradation. Renew Sust Energ Rev 26:521–531. https://doi.org/10.1016/j.rser.2013.06.016
2. Kosseva MR (2013) Chapter 3 - Sources, characterization, and composition of food industry wastes. In: Kosseva MR, Webb C (eds) Food Industry Wastes. Academic Press, San Diego, 37–60. https://doi.org/10.1016/B978-0-12-391921-2.00003-2
3. Alongi M, Melchior S, Anese M (2019) Reducing the glycemic index of short dough biscuits by using apple pomace as a functional ingredient. LWT – Food Sci Technol 100:300–305. https://doi.org/10.1016/j.lwt.2018.10.068

4. Okoro OV, Shavandi A (2021) An assessment of the utilization of waste apple slurry in bio-succinic acid and bioenergy production. Int J Sci Environ Technol. https://doi.org/10.1007/s13762-021-03235-z

5. Ayyachamy M, Cliffe FE, Coyne JM, Collier J, Tuohy MG (2013) Lignin: untapped biopolymers in biomass conversion technologies. Biomass Convers Biorefin 3(3):255–269. https://doi.org/10.1007/s13399-013-0084-4

6. Dhillon GS, Kaur S, Brar SK (2013) Perspective of apple processing wastes as low-cost substrates for bioproduction of high value products: a review. Renew Sust Energ Rev 27:789–805. https://doi.org/10.1016/j.rser.2013.06.046

7. Hobbi P, Okoro OV, Delporte C, Alimoradi H, Podstawczyk D, Nie L, Bernaerts KV, Shavandi A (2021) Kinetic modelling of the solid–liquid extraction process of polyphenolic compounds from apple pomace: influence of solvent composition and temperature. Bioresour Bioprocess 8(1):114. https://doi.org/10.1186/s40643-021-00465-4

8. Zeng J, Yoo CG, Wang F, Pan X, Vermerris W, Tong Z (2015) Biomimetic Fenton-catalyzed lignin depolymerization to high-value aromatics and dicarboxylic acids. Chemsuschem 8(5):861–871. https://doi.org/10.1002/cssc.201403128

9. Asmadi M, Kawamoto H, Saka S (2011) Gas- and solid/liquid-phase reactions during pyrolysis of softwood and hardwood lignins. J Anal Appl Pyrolysis 92(2):417–425. https://doi.org/10.1016/j.jaap.2011.08.003

10. Parsell T, Yohe S, Degenstein J, Jarrell T, Klein I, Gencer E, Hewetson B, Hurt M, Kim JI, Choudhari H, Saha B, Meilan R, Mosier N, Ribeiro F, Delgass WN, Chapple C, Kenttämaa HI, Agrawal R, Abu-Omar MM (2015) A synergistic biorefinery based on catalytic conversion of lignin prior to cellulose starting from lignocellulosic biomass. Green Chem 17(3):1492–1499. https://doi.org/10.1039/C4GC01911C

11. Song Q, Wang F, Cai J, Wang Y, Zhang J, Yu W, Xu J (2013) Lignin depolymerization (LDP) in alcohol over nickel-based catalysts via a fragmentation–hydrogenolysis process. Energy Environ Sci 6(3):994–1007. https://doi.org/10.1039/C2EE23741E

12. Ali OM, Mamat R, Rasul MG, Najafi G (2017) Chapter Eighteen - Potential of biodiesel as fuel for diesel engine. In: Rasul MG, Azad Ak, Sharma SC (eds) Clean Energy Sustain Dev Academic Press, 557–590. https://doi.org/10.1016/B978-0-12-805423-9.00018-1

13. Huang X, Korányi TI, Boot MD, Hensen EJM (2015) Ethanol as capping agent and formaldehyde scavenger for efficient depolymerization of lignin to aromatics. Green Chem 17(11):4941–4950. https://doi.org/10.1039/C5GC01120E

14. Sagues WJ, Bao H, Nemenyi JL, Tong Z (2018) Lignin-first approach to biorefining: utilizing Fenton's reagent and supercritical ethanol for the production of phenolics and sugars. ACS Sustain Chem Eng 6(4):4958–4965. https://doi.org/10.1021/acssuschemeng.7b04500

15. Banerjee G, Car S, Scott-Craig JS, Hodge DB, Walton JD (2011) Alkaline peroxide pretreatment of corn stover: effects of biomass, peroxide, and enzyme loading and composition on yields of glucose and xylose. Biotechnol Biofuels 4(1):16. https://doi.org/10.1186/1754-6834-4-16

16. Cao Z, Dierks M, Clough MT, Daltro de Castro IB, Rinaldi R (2018) A convergent approach for a deep converting lignin-first biorefinery rendering high-energy-density drop-in fuels. Joule 2(6):1118–1133. https://doi.org/10.1016/j.joule.2018.03.012

17. Ouyang X, Huang X, Zhu J, Boot MD, Hensen EJM (2019) Catalytic conversion of lignin in woody biomass into phenolic monomers in methanol/water mixtures without external hydrogen. ACS Sustain Chem Eng 7(16):13764–13773. https://doi.org/10.1021/acssuschemeng.9b01497

18. Rautiainen S, Di Francesco D, Katea SN, Westin G, Tungasmita DN, Samec JSM (2019) Lignin valorization by cobalt-catalyzed fractionation of lignocellulose to yield monophenolic compounds. Chem Sus Chem 12(2):404–408. https://doi.org/10.1002/cssc.201802497

19. Liu Y, Li C, Miao W, Tang W, Xue D, Xiao J, Zhang T, Wang C (2020) Rhodium-terpyridine catalyzed redox-neutral depolymerization of lignin in water. Green Chem 22(1):33–38. https://doi.org/10.1039/C9GC03057C

20. Graça I, Woodward RT, Kennema M, Rinaldi R (2018) Formation and fate of carboxylic acids in the lignin-first biorefining of lignocellulose via H-transfer catalyzed by Raney Ni. ACS Sustain Chem Eng 6(10):13408–13419. https://doi.org/10.1021/acssuschemeng.8b03190

21. Guo T, Li X, Liu X, Guo Y, Wang Y (2018) Catalytic transformation of lignocellulosic biomass into arenes, 5-hydroxymethylfurfural, and furfural. Chemsuschem 11(16):2758–2765. https://doi.org/10.1002/cssc.201800967

22. Liu X, Li H, Xiao L-P, Sun R-C, Song G (2019) Chemodivergent hydrogenolysis of eucalyptus lignin with Ni@ZIF-8 catalyst. Green Chem 21(6):1498–1504. https://doi.org/10.1039/C8GC03511C

23. Thornburg NE, Pecha MB, Brandner DG, Reed ML, Vermaas JV, Michener WE, Katahira R, Vinzant TB, Foust TD, Donohoe BS, Román-Leshkov Y, Ciesielski PN, Beckham GT (2020) Mesoscale reaction–diffusion phenomena governing lignin-first biomass fractionation. Chemsuschem 13(17):4495–4509. https://doi.org/10.1002/cssc.202000558

24. Luo H, Klein IM, Jiang Y, Zhu H, Liu B, Kenttämaa HI, Abu-Omar MM (2016) Total utilization of miscanthus biomass, lignin and carbohydrates, using earth abundant nickel catalyst. ACS Sustain Chem Eng 4(4):2316–2322. https://doi.org/10.1021/acssuschemeng.5b01776

25. Chisti Y (2019) Chapter 1 - Introduction to algal fuels. In: Pandey A, Chang J-S, Soccol CR, Lee D-J, Chisti Y (eds) Biofuels from Algae (Second Edition). Elsevier, 1–31. https://doi.org/10.1016/B978-0-444-64192-2.00001-9

26. Chen Y, Wu Y, Hua D, Li C, Harold MP, Wang J, Yang M (2015) Thermochemical conversion of low-lipid microalgae for the production of liquid fuels: challenges and opportunities. RSC Adv 5(24):18673–18701. https://doi.org/10.1039/C4RA13359E

27. Obeid R, Lewis DM, Smith N, Hall T, van Eyk P (2020) Reaction kinetics and characterisation of species in renewable crude from hydrothermal liquefaction of monomers to represent organic fractions of biomass feedstocks. Chem Eng J 389:124397. https://doi.org/10.1016/j.cej.2020.124397

28. Rao JS, Kumar B (2012) 3D Blade root shape optimization. 10th International Conference on Vibrations in Rotating Machinery. Woodhead Publishing, 173–188. https://doi.org/10.1533/9780857094537.4.173

29. Mohammadi R, Mohammadifar MA, Mortazavian AM, Rouhi M, Ghasemi JB, Delshadian Z (2016) Extraction optimization of pepsin-soluble collagen from eggshell membrane by response surface methodology (RSM). Food Chem 190:186–193. https://doi.org/10.1016/j.foodchem.2015.05.073

30. Roosta M, Ghaedi M, Asfaram A (2015) Simultaneous ultrasonic-assisted removal of malachite green and safranin O by copper nanowires loaded on activated carbon: central composite design optimization. RSC Adv 5(70):57021–57029. https://doi.org/10.1039/C5RA03519H

31. Halim NAA, Abidin ZZ, Siajam SI, Hean CG, Harun MR (2021) Optimization studies and compositional analysis of subcritical water extraction of essential oil from Citrus hystrix DC. leaves. J Supercrit Fluids 178. https://doi.org/10.1016/j.supflu.2021.105384

32. Anderson EM, Stone ML, Hülsey MJ, Beckham GT, Román-Leshkov Y (2018) Kinetic studies of lignin solvolysis and reduction by reductive catalytic fractionation decoupled in flow-through reactors. ACS Sustain Chem Eng 6(6):7951–7959. https://doi.org/10.1021/acssuschemeng.8b01256

33. Okoro OV, Sun Z, Birch J (2017) Meat processing dissolved air flotation sludge as a potential biodiesel feedstock in New Zealand: A predictive analysis of the biodiesel product properties. J Clean Prod 168:1436–1447. https://doi.org/10.1016/j.jclepro.2017.09.128

34. Okoro OV, Sun Z, Birch J (2019) 10 - Thermal depolymerization of biogas digestate as a viable digestate processing and resource recovery strategy. In: Azad K (ed) Advances in Eco-Fuels for a Sustainable Environment. Woodhead Publishing, 277–308. https://doi.org/10.1016/B978-0-08-102728-8.00010-3

35. Jones S, Zhu Y, Anderson D, Hallen R, Elliot D, Schmidt A, Albrecht K, Hart T, Butcher M, Drennan C, Snowden-Swan L, Davis R, Kinchin C (2014) Process design and economics for the conversion of algal biomass to hydrocarbons: whole algae hydrothermal liquefaction and upgrading. Pacific Northwest National laboratory, Springfield

36. Shalini R, Gupta DK (2010) Utilization of pomace from apple processing industries: a review. J Food Sci Technol 47(4):365–371. https://doi.org/10.1007/s13197-010-0061-x

37. AACE International (2011) Recommended practice no. 59R-10, development of factoredcost estimates – as applied In Engineering, Procurement, And Construction For The ProcessIndustries. AACE International. Morgantown

38. Towler G, Sinnott G (2008) Chemical engineering design: Principles, practice and economics of plant process design. Elsevier, London

39. Sudha ML, Baskaran V, Leelavathi K (2007) Apple pomace as a source of dietary fiber and polyphenols and its effect on the rheological characteristics and cake making. Food Chem 104(2):686–692. https://doi.org/10.1016/j.foodchem.2006.12.016

40. Bartels JR (2008) A feasibility study of implementing an Ammonia Economy. Iowa State University

41. Okoro OV, Sun Z, Birch J (2018) Prognostic Assessment of the Viability of Hydrothermal Liquefaction as a Post-Resource Recovery Step after Enhanced Biomethane Generation Using Co-Digestion Technologies. Appl Sci 8(11):2290

42. Minowa T, Kondo TaS ST (1998) Thermochemical liquefaction of indonesian biomass residues. Biomass Bioenergy 14(5/6):517–524

43. Vogel HG (2014) Process development: from the initial idea to the chemical production plant. Wiley, Weinheim

44. Braun MR, Altan H, Beck SBM (2014) Using regression analysis to predict the future energy consumption of a supermarket in the UK. Appl Energy 130:305–313. https://doi.org/10.1016/j.apenergy.2014.05.062

45. Lu J, Boughner EC, Liotta CL, Eckert CA (2002) Nearcritical and supercritical ethanol as a benign solvent: polarity and hydrogen-bonding. Fluid Phase Equilib 198(1):37–49. https://doi.org/10.1016/S0378-3812(01)00754-3

46. Perez-Benito JF (2004) Iron(III)−Hydrogen peroxide reaction: kinetic evidence of a hydroxyl-mediated chain mechanism. The J Phys Chem A 108(22):4853–4858. https://doi.org/10.1021/jp031339l

47. Okoro O, Sun Z, Birch J (2018) Catalyst-free biodiesel production methods: a comparative technical and environmental evaluation. Sustain 10(2):127. https://doi.org/10.3390/su10010127

48. Brand S, Susanti RF, Kim SK, Lee H-s, Kim J, Sang B-I (2013) Supercritical ethanol as an enhanced medium for lignocellulosic biomass liquefaction: Influence of physical process parameters. Energy 59:173–182. https://doi.org/10.1016/j.energy.2013.06.049

49. Wu X-F, Zhang J-J, Huang Y-H, Li M-F, Bian J, Peng F (2019) Comparative investigation on bio-oil production from eucalyptus via liquefaction in subcritical water and supercritical ethanol. Ind Crops Prod 140:111695. https://doi.org/10.1016/j.indcrop.2019.111695

50. Okoro OV, Sun Z (2021) The characterisation of biochar and biocrude products of the hydrothermal liquefaction of raw digestate biomass. Biomass Convers Biorefin 11(6):2947–2961. https://doi.org/10.1007/s13399-020-00672-7

51. Chen M-Y, Huang Y-B, Pang H, Liu X-X, Fu Y (2015) Hydrodeoxygenation of lignin-derived phenols into alkanes over carbon nanotube supported Ru catalysts in biphasic systems. Green Chem 17(3):1710–1717. https://doi.org/10.1039/C4GC01992J